RevMexAA (Serie de Conferencias), **41**, 5–11 (2011)

THE CLIMATE OF NORTHERN CHILE: MEAN STATE, VARIABILITY AND TRENDS

R. D. Garreaud[1]

RESUMEN

Este manuscrito documenta las características principales del clima del norte de Chile, lugar donde se ubican, y donde se proyecta, la instalación de varios observatorios astronómicos. Primeramente se provee de una descripción del clima regional a una escala espacial amplia, donde se describe la importancia relativa de la celda de Hadley, del Monsón Sud-Americano, y perturbaciones extra-tropicales en dar forma al estado promedio de la temperatura, precipitación y vientos en la región. Entonces, se describen los efectos de la Oscilación del Sur-El Niño para producir algún nivel de variabilidad inter-anual en el clima del norte de Chile. Se concluye este trabajo, basándose en lo expuesto en estudios recientes, con un resumen de las tendencias observadas y proyecciones en el cambio climático para lo que resta del siglo XXI.

ABSTRACT

This paper documents the main features of the climate of northern Chile where several astronomical observatories are located or projected to be built. We first provide a large-scale context for the regional climate, describing the relative importance of the Hadley cell, South American Monsoon and extratropical disturbances in shaping the mean state of temperature, precipitation and winds. We then describe the effects of the El Niño-Southern Oscillation in producing some level of interannual variability in northern Chile and conclude our work summarizing recent studies on observed climate trends and projected climate changes during the rest of the 21^{st} century.

Key Words: atmospheric effects — site testing

1. PRESENTATION

Loosely speaking, northern Chile is the narrow strip of land (∼300 km) between the Andean ridge and the Pacific coast extending meridionally from about 18°–30°S (Figure 1). Consistent with its subtropical location and the presence of the cold waters of immediately to the west, northern Chile features an extremely arid climate characterized by of lack of precipitation, very low humidity and, generally, absence of clouds. Given these favourable conditions for astronomical observations, a relative large number of astronomical facilities are located in northern Chile (Figure 1). In spite of its aridity and stability, the regional climate does exhibit significant spatial variability (especially in the east-west direction), as well as interannual fluctuations (climate variability) and long-term trends (climate change). In this work, we offer a brief review of the northern Chile climate, emphasizing the physical processes that explain its mean state (§ 2) and variability (§§ 3 and 4). We hope that such review will provide a large-scale, longer-period context for the contributions dealing with more specific climatic features that are relevant for the planning and management of the astronomical observatories in this region.

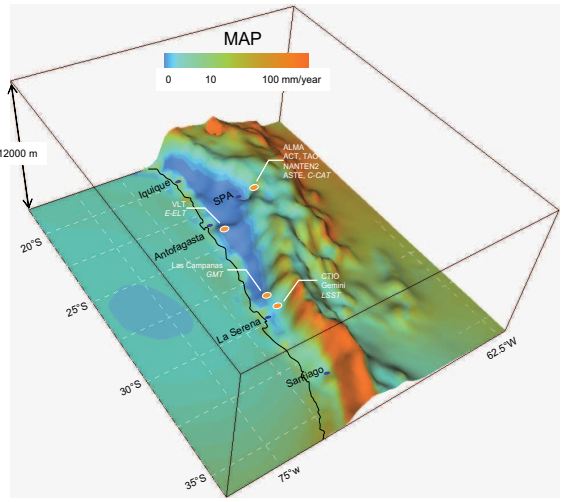

Fig. 1. Annual mean precipitation (colors) displayed over the terrain elevation of north-central Chile. Also shown are major cities (blue circles) and cluster of astronomical observatories (yellow circles).

[1]Department of Geophysics, Universidad de Chile, Blanco Encalada 2002, Santiago, Chile (rgarreau@dgf.uchile.cl).

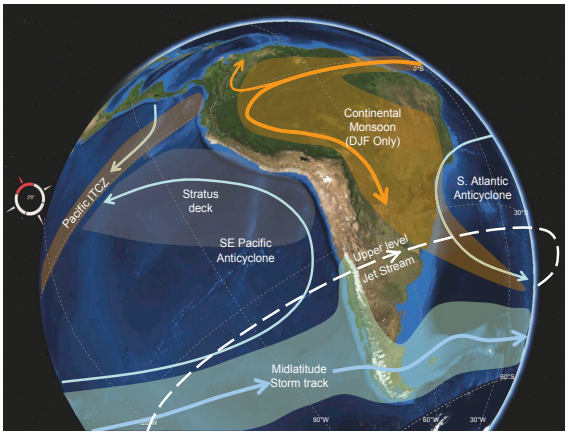

Fig. 2. Schematics of the low-level (below 1 km) circulation over South America (solid arrows), main precipitation systems and stratus cloud deck (shaded areas), and the upper-level westerly jet stream (dashed arrow).

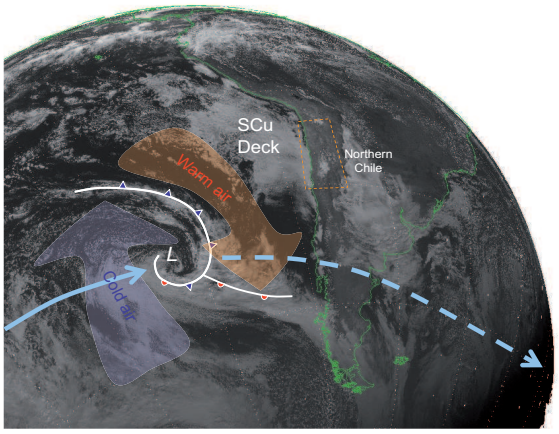

Fig. 3. A GOES-13 visible image (14UTC, 30-05-2011) depicting a frontal system (white lines) formed around a surface low pressure center (denoted by a letter L). The low has followed the solid blue line and it is likely to continue moving to the east along the dashed blue line. The wide blue and yellow arrows indicate the low-level air movement around the low. Also evident in this figure is the deck of stratocumulus (SCu), thin, low-level, non-precipitating clouds usually formed atop of the AMBL over the SE Pacific.

2. CLIMATE BACKGROUND

2.1. *Continental-scale condition*

Figure 2 schematizes the main large-scale, near-surface circulation features over South America and the adjacent oceans. Over the tropical Pacific there is intense precipitation produced by the convergence of the trade winds into the thermal equator (referred as the Intertropical Convergence Zone, ITCZ). The air is forced to ascend, loosing most of its moisture, until reaching the tropical tropopause (∼15 km ASL) and then diverge toward the poles at each hemisphere. A Hadley cell is closed by the slow descend of air (subsidence) at subtropical latitudes in each hemisphere. Subsidence maintains the Southeast (SE) Pacific anticyclone (high pressure at the surface), warms the middle- and lower troposphere and brings dry air, the key ingredients explaining the arid or semi-arid climates that prevail at subtropical latitudes. The extent, position and strength of the Hadley cells vary with the seasons. During austral summer (DJF) the SE Pacific anticyclone is slightly weaker but reaches its southernmost position, producing stable, dry conditions down to south-central Chile. In austral winter (JJA) the anticyclone is more intense but retracts into the subtropics.

The SE Pacific anticyclone is separated from its counterpart over the South Atlantic by an area of relatively low pressure over the interior of the continent that prevail year round. Increased insolation during spring rapidly warms the land deepening the continental low and forcing low-level flow from the Amazon basin toward the south. The water vapour transported by this low-level jet feeds copious rain from the Amazon basin towards La Plata basin (Figure 2) in which is now referred to as the South American Monsoon System (e.g., Vera et al. 2010). Note that northern Chile remains isolated from the Monsoon regime with the Andes cordillera in between. Nevertheless, the arid conditions in northern Chile are not primarily caused by the Andes (supposedly blocking the moist air from the east) but rather by its subtropical latitudes and presence of cold waters in the Pacific (Garreaud et al. 2010), as described in detail in the next section.

The air diverging from the ITCZ in the upper troposphere is deflected eastward by the effect of the earth rotation, leading to troposheric-deep westerly flow at midlatitudes that maximize in a circumpolar jet stream (wind speed >40 m/s) at 10–12 km ASL (Figure 2). The jet signals a strong contrast in air temperature and its dynamic instability produces the sequence of high and low pressure centers that characterize the extratropical Rossby regime. These centers tend to move eastward along a zonal band known as the storm track at about 45°–55°S in the Southern Hemisphere. Of particular relevance is the development of deep stratiform clouds and precipitation along the cold fronts, rooted in the low-pressure centres and arching into subtropical latitudes (Fig-

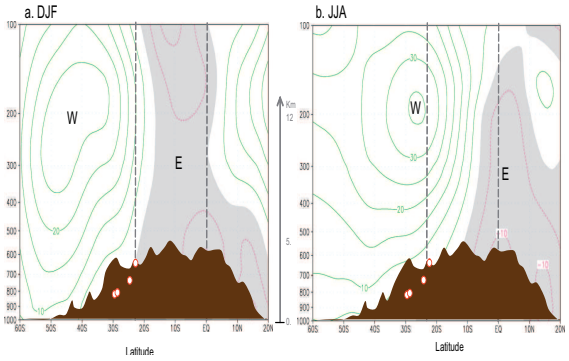

Fig. 4. Pressure/height-latitude cross section of the long-term mean zonal (west-east) wind at 80W (a few hundreds of km off the Chilean coast) for (a) austral summer (DJF) and (b) austral winter (JJA). Contour interval is +10 m/s or −5 m/s. Areas with easterly flow (U<0) are shown in grey. Brown area indicates mean Andean height. For reference, small white circles indicate the approximate position of CTIO, Gemini, VLT and ALMA.

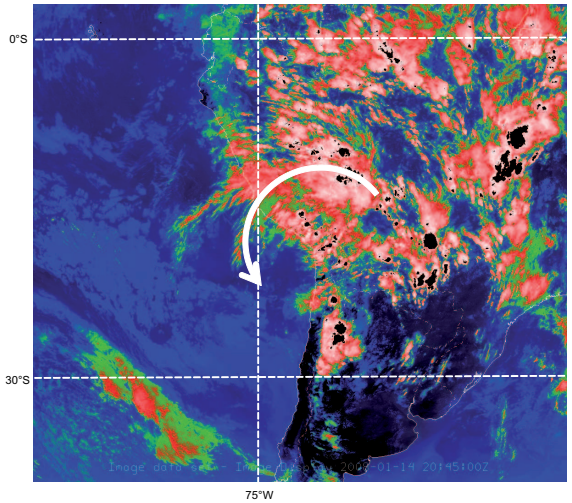

Fig. 5. A GOES-13 Infrared image (20:45 UTC 14-01-2008). The color scale indicates brightness temperature with the following interpreration: black = continental cloud free areas; dark blue = ocean cloud free areas; light blue = shallow clouds areas; green to red to pink= deep, convective clouds. Note the widespread area of deep convection over the central part of the continent and the central Andes. The Bolivian high (siganled by the white arrow) is capable to extend some cirrus (also seen in green and red colors) thousands of km away from the area of convection, thus reaching the SE Pacific.

ure 3), resulting in a secondary maximum of precipitation at midlatitudes (Figure 2). The presence of the Andes cordillera enhances precipitation along its western slope and extends the area of precipitation up to central Chile producing a significant snow pack as north as 30S during austral winter.

To further describe the circulation at upper levels, Figures 4a,b show the seasonal mean zonal flow in a latitude-height cross section at 80°W (a few hundreds km off the northern Chilean coast). Westerly winds (flow from the Pacific to the continent, generally bringing dry air) prevail in the whole troposphere at midlatitudes, while easterly winds (flow from the continent to the Pacific, generally bringing moist air) prevail at lower latitudes. During austral summer, the axis of the westerly jet stream is at 45°S and the tropical easterlies reaches down to 20°S, affecting the central Andes and the South American Altiplano. The mid- and upper-level easterlies over the central Andes are due to the seasonal establishment of the Bolivian high, an upper-level anticyclone associated with the South American Monsoon (Figure 5). In austral winter, the whole wind system displaces northward, with the westerly winds reaching 10°S and the jet axis at 25°S. Note that the cluster of astronomical observatories in northernmost Chile does experience a seasonal change in the mid- and upper-level zonal flow.

2.2. *Mean conditions over northern Chile*

As stated before, northern Chile and southern Per exhibits a very arid climate, including the Atacama dessert, arguable the driest place on earth, with mean precipitation as low as 10 mm per decade (Figure 1). While large-scale subsidence at subtropical latitudes is the primary cause of aridity, other factors must be at play to produce such extreme conditions, including the adjacent cold ocean and the Andean slope (Rutllant et al. 2003; Garreaud et al. 2010). The SE Pacific anticyclone drives persistent southerly winds along the Chilean coast, which in turns forces upwelling of cold waters in that region. The adiabatically warmed air aloft and the cold air in contact with the sea surface results in a thermal inversion depicted by the vertical profiles of the average air temperature and dew point temperature in Figure 6 at Antofagasta (coastal site at 23.5°S) for winter and summer. The air temperature decreases in the atmospheric marine boundary layer (AMBL), about 800 m deep, followed by a layer in which the temperature increases more than 5°C. Above this temperature inversion (TI) the air temperature cools again in the free troposphere (FT). Compared with the summer conditions, the AMBL is about 5°C cooler, the AMBL is about 200 m shallower, and the temperature increase across the inversion is about

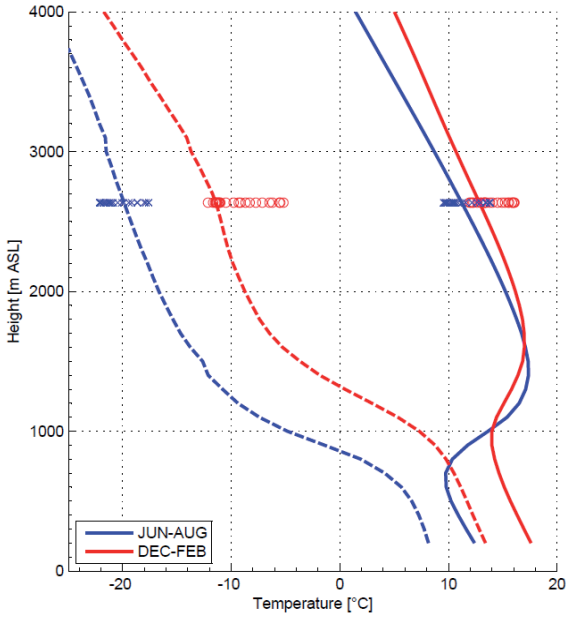

Fig. 6. Vertical profiles of air temperature (Ta, solid lines) and dew point temperature (Td, dashed lines) obtained from the radiosonde launched at Antofagasta (23.5°S, 70.2°W). The daily data (at 12:00 UTC) was averaged for winter (JJA, blue) and summer (DJF, red) from 1978–2009. Recall that Ta-Td is a moisture parameter, as the difference decreases (increases) for moist (dry) air. The crosses and circles at 2600 m indicate the hourly mean values of Ta and Td measures at 2-m in the Paranal observatory. Note how close are these near-surface values to the free-tropospheric air at the same level.

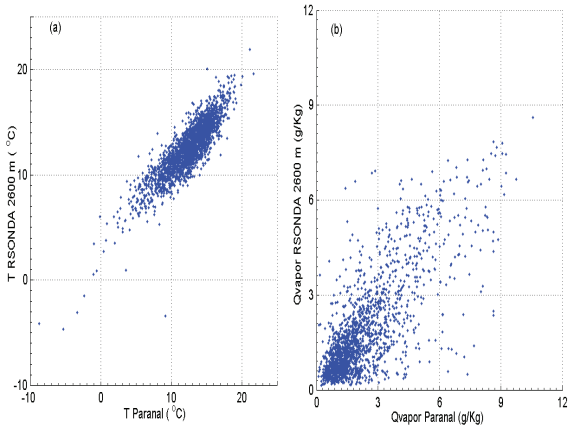

Fig. 7. (a) Scatter plot of daily values (measured at 1200 UTC) of air temperature at 2 m above the surface recorded at Paranal and in the free-troposphere at 2600 m ASL measured by the Antofagasta radiosonde (2600 m is approximately the height of the weather station at Paranal). (b) Same as panel (a) but for water vapour mixing ratio.

3°C higher. Even a customary examination of individual profiles at Antofagasta reveals that such AMBL-TI-FT structure is present almost every day (Muñoz et al. 2011; Rahn & Garreaud 2010) albeit with shaper features. The dew-point temperature profile reveals moist air in the AMBL, which is often capped by a thin layer of stratus clouds, followed by extremely dry air (relative humdity <15%; water vapour mixing ratio <3 g/Kg) aloft. The stratus clouds over Antofagasta are more prevalent in winter (when the inversion is sharper) and they blanket most of the SE subtropical Pacific (e.g., Figure 3; see Painemal et al. 2010 for stratus climatology).

Because northern Chile exhibits a very sharp and almost continuous coastal escarpment, with terrain elevation rising from sea level to about 1000 m ASL within 10–20 km from the coast line, the moist, cool air in the AMBL is laterally restricted also, and FT dry air prevails inland. Of course, over the Atacama Desert, the daily cycle of surface heating/cooling results in the development of daytime dry mixed layer and a very marked nocturnal inversion. Nevertheless, the air conditions in the observatories located atop of the coastal mountains and further inland are quite similar to the free tropospheric air at the same level, as shown by the seasonal mean range of the 2 m air temperature and dew point at Paranal (Figure 6). Not only the mean conditions at Paranal are similar to their counterparts in the FT, but also their day-to-day variations are highly correlated (Figure 7), indicative of a high degree of co-variability between local surface and FT conditions.

As ones moves farther to the east, the effect of the Andes cordillera becomes more prominent. Strong upslope wind blows during daytime (especially in summer), while equally strong down slope wind (katabatic flow) blows during night (especially in winter) (Rutllant et al. 2003). The transition between upslope and downslope flow implies strong wind shear, eventually increasing the low-level mechanical turbulence. The Andes also blocks the large-scale westerly flow (c.f. Figure 4) resulting in winds blowing from the north in the vicinity of the cordillera (Figure 8) below its crest level. Near the top of the Andes (say, stations over 5000 m ASL) the local wind will become closer to the FT flow (see Figure 4). The FT air in the western slope of the Andes is generally dry because it originates in the Pacific

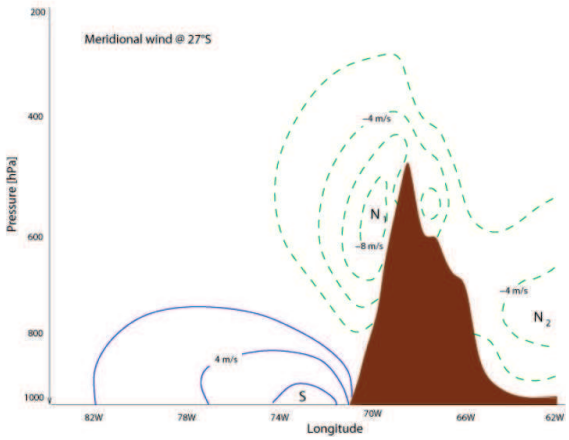

Fig. 8. Pressure-longitude cross section of the meridional wind at 27°S during austral spring (SON). Contour interval is 2 m/s, the zero line is omitted and negative values in dashed lines. The brown area represents the Andes profile at this latitude. To the west of the Andes there is a southerly low-level jet (signalled by an S) just off the coast and a northerly jet (signalled by N1) close to the Andean slope. To the east of the Andes there is evidence of the northerly low-level jet (signalled by N2). Data source: PRECIS simulation of the present day climate.

above the AMBL, but to the north of 23°S easterly winds occasionally occurs during austral summer bringing tongues of moist air from the interior of the continent above 4000 m ASL (e.g., Falvey & Garreaud 2005). During periods of active convection over the Altiplano it is also possible the presence of high clouds and precipitation spill-over causing rainfall events in the Andes foothills (Figure 5).

3. CLIMATE VARIABILITY

The general circulation of the atmosphere can be disturbed by large-scale phenomena that arise from instability of the coupled atmosphere-ocean system (also referred as internal modes). By far, the most important of these modes is the El Niño-Southern Oscillation (ENSO) that oscillates between two extreme phases (El Niño and La Niña) with an irregular period between 2 and 7 years. ENSO is rooted in the tropical Pacific, affecting directly the nearby areas (e.g., tropical South America) but by modifying the central Pacific ITCZ it is also capable to alter the upper-level jet stream and thus the extratropical storm tracks. Indeed, a significant fraction of the year-to-year variability of the air temperature, precipitation and wind across much of South America (and elsewhere) is associated with ENSO variations (see Garreaud & Falvey 2009 for a review). Other large-scale internal modes include the Pacific Decadal Oscillation and the annular modes at higher latitudes, explaining some of the inter-decadal and longer-term variability of meteorological conditions.

One can estimate the influence of ENSO in the year-to-year variability of some variable (e.g., the seeing) at a particular site by calculating the correlation between the variable itself and an ENSO index. Such task is beyond the scope of this review and here we only describe the ENSO impact on large scale circulation features that might be relevant to astronomical observations in northern Chile. Let us summarize the main anomalies (departures with respect to climatology) during an El Niño event (EN); anomalies during a La Niña event are roughly the inverse to those described here.

- The warming of the tropical Pacific is directly sensed by the near surface air along Pacific coast of South America as far south as 30°S. During a strong EN year the AMBL off northern Chile can warms up as much as 2°C, but there is no major changes in the inversion base height that remain close to 1000 m ASL. Farther aloft there is also a tendency for warmer temperatures.
- During EN years there is a general intensification of the westerly flow aloft at subtropical latitudes, including a strengthening of the jet stream crossing the Andes at about 25°S during winter (c.f. Fig. Xa). The stronger than normal wind aloft may produce higher mechanical turbulence above northern Chile. On the other hand, stronger westerlies reduce the transport of moist air above the central Andes and limit the precipitation over the Altiplano during summer (e.g., Garreaud & Aceituno 2001).
- The weakening of the subtropical SE Pacific anticyclone is one of the key ingredients of an EN event. This, in concert with a stronger jet stream aloft and a frequent occurrence of blocking anticyclones in the austral Pacific is capable of a northward shift of the midlatitude storm track, bringing more storms and winter precipitation to central Chile (30°–37°S) than in an average year. For instance, the average precipitation in La Serena (30°S) is about 100 mm per year (most of it concentrated in JJA) but can reach up to 300 mm during strong EN events (e.g., Montecinos & Aceituno 2003).

4. CLIMATE CHANGE

4.1. *Observed Trends*

Many of the climate trends observed during the past century worldwide have been attributed to the

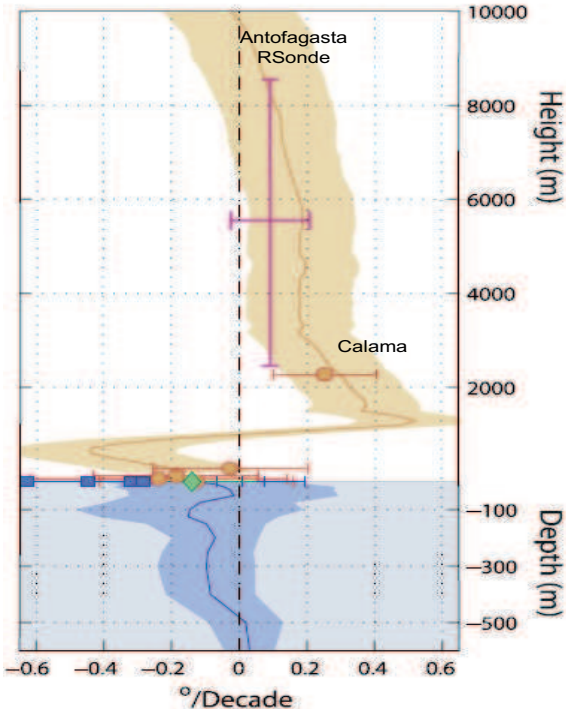

Fig. 9. Vertical profiles of temperature trends (°C/decade) in northern Chile from 1979 to 2005. The upper (lower) portion of the graph represents the atmosphere (ocean). The solid lines are the Antofagasta radiosonde derived trends and ligther shaded region indicates the 90% confidence interval. Orange circles and blue squares represent temperature trends derived from the in-situ measurements of air temperature and sea-surface temperature, along with their 90% confidence interval (horizontal bars). Ocean temperature trends (blue) derived from the World Ocean Dataset. Adapted from Falvey & Garreaud (2009).

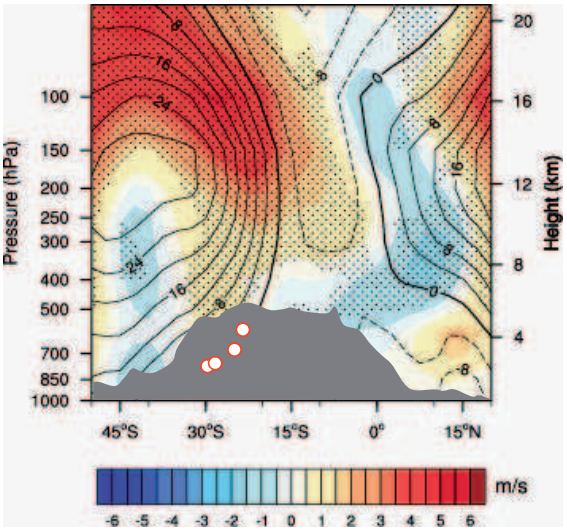

Fig. 10. Black contours indicate the DJF zonal wind mean (in m s^{-1}) across the 70°W section over the 1970–1999 period. The average is based in an ensemble of 11 GCMs run for the IPCC 4th Assessment report. In colors, multimodel mean difference (in m s^{-1}) of summer DJF U200 across the 70W section between the 2070–2099 (under the A2 scenario) and 1970–1999 periods. Little black points indicate where more than 9 models agree on the sign of the difference. Note the significant increase in the westerly flow by the end of the 21st century. Adapted from Minvielle & Garreaud (2011). For reference, small white circles indicate the approximate position of CTIO, Gemini, VLT and ALMA.

increase in concentration of greenhouse gases (mostly CO2 and Methane) emitted by human activities (fossil fuel burning, massive agriculture and deforestation). The icon of this anthropogenic climate change is the ∼1°C increase in global mean surface air temperature between 1900s and present day, along with a decline in snow cover in the Northern Hemisphere and sea level rise (Christensen et al. 2007). Nevertheless, the spatial patterns of the temperature changes exhibits considerable spatial variability because of changes in atmospheric circulation induced by the greenhouse effect itself and the existence of natural modes whose amplitude over interdecadal timescales is comparable to the anthropogenic signal. Using in-situ, radiosonde and satellite information from 1979 onwards, Falvey & Garreaud (2009) found a marked cooling (−0.25°/decade) along the coast of north-central Chile, presumably because the increase in upwelling-favorable southerly winds, contrasting with a marked warming (+0.25°/decade) inland and over the Andean slope (Figure 9). Unfortunately, the climatological network in Chile is sparse and the highest station in the north (Calama) is only at 2200 m ASL, hindering our diagnosis of any potential changes occurring closer to the astronomical observatories. The coastal areas and the inland dessert havent experienced any increase in precipitation and up-to-date, there is no evidence of significant precipitation or moisture changes in the central Andes (Haylock et al. 2006).

4.2. *Climate change projections*

Insights of the climate change during the 21st century are obtained from numerical global circulation models (GCMs) of the atmosphere, forced by a suite of projections of greenhouse gasses concentration referred to as concentration scenarios. One

often examines the A2 scenario (worst case) in which the CO2 concentration increases from current values around 360 ppm to about 820 ppm by the end of the century. Under this scenario, the GCMs predict a consistent free-tropospheric warming as high as +5°C over northern Chile and the central Andes (Bradley et al. 2008). Similar increase in temperature is expected close to the surface over the Atacama Desert and the central Andes. The coastal AMBL would warm 1–2°C only because of the larger thermal inertia of the ocean and a possible increase of the upwelling-favorable southerly winds that tend to offset the radiative warming (Garreaud & Falvey 2009). Thus, the warming aloft and the near-ocean cooling could probably result in a stronger temperature inversion, confining more effectively the moist air in the coastal AMBL.

When examining the projected changes in free-tropospheric wind (a reliable output from GCMs), Minvielle & Garreaud (2011) found an almost year-round increase in westerly flow at middle- and upper-levels over the subtropical South America (Figure 10). That results in (a) stronger westerly winds aloft crossing northern Chile in winter, and (b) a decrease of the moisture transport towards the central Andes from the interior of the continent during summer. The later would reduce the summer precipitation over the Altiplano between 10–30% relative to current values (Minvielle & Garreaud 2011).

To the south of 30°S the GCM predicted changes in air temperature tend to be smaller (+2°C to +3°C), but there is a consistent signal of drying in south-central Chile (Fuenzalida et al. 2007). Under scenario A2, the precipitation by the end of the century would be 50–70% of current values between Santiago and Puerto Montt because of a southward shift of the storm track.

This work was motivated by an invitation to present a talk at the Conference Astronomical Site Testing Data in Chile hosted by the Universidad de Valparaíso in December 2010, and further encouraged by Angel Otárola and Michel Curé. Data and scripts for Figures 6 and 7 were kindly provided by Dr. Ricardo Muñoz.

REFERENCES

Bradley, R. S., Vuille, M., Diaz, H. F, & Vergara, W. 2008, Science, 312, 1755

Christensen, J. H., et al. 2007, in Climate Change 2007: The Physical Science Basis, ed. S. Solomon, D. Qin, M. Manning, Z. Chen, M. Marquis, K. B. Averyt, M. Tignor & H.L. Miller (Cambridge: Cambridge Univ. Press)

Falvey, M., & Garreaud, R. 2005, J. Geophys. Res., 110, D22105

_____. 2009, J. Geophys. Res., 114, D04102

Fuenzalida, H., Aceituno, P., Falvey, M., Garreaud, R., Rojas, M., & Sanchez, R.2007, Study on Climate Variability for Chile during the 21st century, Technical Report for the National Environmental Committee (`http://www.dgf.uchile.cl/PRECIS`)

Garreaud, R. D., & Aceituno, P. 2001, J. Climate, 14, 2779

Garreaud, R., & Falvey, M. 2009, Int. J. Climatology, 29, 543

Garreaud, R., Molina, A., & Farias, M. 2010, Earth Planetary Sci. Lett., 292, 39

Haylock, M., et al. 2006, J. Climate, 19, 1490

Minvielle, M., & Garreaud, R. 2011, J. Climate, 24, 4577

Montecinos, A., & Aceituno, P. 2003, J. Climate, 16, 281

Muñoz, R. C., Zamora, R. A., & Rutllant, J. A. 2011, J. Climate, 24, 1013

Painemal, D., Garreaud, R., Rutllant, J., & Zuidema, P. 2010, J. Appl. Meteorol. Clim., 49, 463

Rahn, D., & Garreaud, R. 2010, Atmos. Chem. Phys., 10, 4491